Materials Physics and Mechanics. 2022;48(3): 407-418
Research article
http://dx.doi.org/10.18149/MPM.4832022_11

Submitted: February 9, 2022
Approved: May 23, 2022
Accepted: June 2, 2022

An out-of-plane oscillating beam nanoresonator with ultrahigh intrinsic quality factor

Chu Manh Hoang[1]✉, Nguyen Van Duong[2], Dang Van Hieu[2]

[1]International Training Institute for Materials Science, Hanoi University of Science and Technology, No. 1, Dai Co Viet, Hai Ba Trung, Hanoi, Viet Nam

[2]FPT University, Hoa Lac High Tech Park, Hanoi, Viet Nam

✉ hoangcm@itims.edu.vn, hoang.chumanh@hust.edu.vn

Abstract. An out-of-plane oscillating beam nanoresonator with the ultrahigh intrinsic quality factor based on the motion transformation mechanism from torsion into rotation is reported. The nanoresonator is composed of two resonant beams which are mechanically coupled through two spring beams oscillating in an out-of-phase torsional mode. The out-of-phase torsional oscillation of the two spring beams forms a stationary point in the middle of a supporting beam, which minimizes anchor loss. The low thermoelastic damping (TED) in the nanoresonator is obtained by employing the torsional oscillation mode. The optimal study for minimizing TED has been carried out by varying the representative geometry parameters of the nanoresonator. The nanoresonator with a quality factor over 10^7 has been obtained by the proposed oscillation excitation method.

Keywords: beam nanoresonator, out-of-plane oscillation, torsional oscillation, thermoelastic damping

Acknowledgements*. This work is financially supported by the Vietnam Ministry of Education and Training, Project number B2020-BKA-23-CTVL.*

Citation: Hoang CM, Duong NV, Hieu DV. An out-of-plane oscillating beam nanoresonator with ultrahigh intrinsic quality factor. *Materials Physics and Mechanics*. 2022;48(3): 407-418. DOI: 10.18149/MPM.4832022_11.

1. Introduction

Mechanical resonators have recently attracted much interest because of their wide range of applications in sensing, timing, and physical measurements [1-5]. An important parameter for the performance evaluation of mechanical resonators is the quality factor (Q). A resonator with a high Q implies a higher sensitivity in sensors, a good frequency resolution in filters, and low phase noise in oscillators. In order to maximize Q, it is fundamental to understand physical mechanisms limiting Q. Physical mechanisms of energy dissipation can be described by two categories: extrinsic and intrinsic losses [6-12]. The extrinsic losses are acoustic radiation, surface loss, and air friction, while the intrinsic losses include material loss, anchor loss, and thermoelastic damping (TED). Besides, the operation modes and imperfection of resonators/attached masses also affect the factor Q [8,9,11]. Under low vacuum conditions, losses in mechanical resonators are often generated from extrinsic damping mechanisms such as air damping [6-12]. Under high vacuum conditions, extrinsic dampings become negligible, and intrinsic damping mechanisms such as anchor loss and TED need to be taken into account.

Anchor loss is often dominanted by the radiation of elastic energy through anchors to the substrate [13,14]. This loss can be eliminated by using virtual supports [15] or by connecting the beam to the nodal points of spring beams [16]. Anchor loss can also be reduced by using extensional mode resonators [17]. Recent research have also been conducted on TED that shows to be another intrinsic damping source affecting the upper limit of Q [18-21]. The TED damping relates to the irreversible process of heat flow generated by compressed and extended regions between various parts of an oscillation structure [19-21]. For a material having a positive coefficient of thermal expansion, the compression in an oscillation structure leads to a higher temperature region while the tensile stress on its opposite side results in a lower temperature region. The strength of TED depends on the oscillation frequency, the relevant thermal relaxation time constant, and on the stress distribution in the oscillation structure. These, in turn, depend on the structural geometry and also on the material properties which are themselves functions of temperature. Resonators with high Q values can be obtained by operating the device at a low temperature [22]. Recently, engineered resonators for reducing TED have also been introduced [22-28]. These resonators can be in-plane flexural oscillation or out-of-plane oscillation. In a recent study [16], a flexural free-free resonator is studied and the TED Q has obtained around 10^6. The numerical evaluation of TED in microelectromechanical systems has been reported [29], in which the numerical results on TED of the flexural free-fixed beam resonators have been compared with analytical solutions [19]. To obtain a high Q resonator, it is necessary to consider not only anchor loss but also TED. The TED dissipation is generated from the extension and compression in the flexural vibrations of the mechanical resonator. Several out-of-plane (OP) vibrational resonators have been reported [26-28]. However, an OP vibrational beam nanoresonator operating in the MHz regime with the ultrahigh intrinsic Q in considering both anchor loss and TED has not yet been studied with much interest and needs to be reported.

In this paper, we propose an OP vibrational beam nanoresonator. The OP vibration is carried out by the motion transformation from torsion into rotation. The application of the torsional oscillation mode is to minimize TED, while the out-of-phase oscillation is to suppress energy dissipation caused by anchor loss. Anchor loss is first investigated by decomposing the structure of the nanoresonator. Then, TED in the nanoresonator depending on its representative geometry parameters is investigated in detail. The Q-factor of the nanoresonator is optimized by considering the design of the cross-section and aspect ratio of the beams to minimize TED. The dependence of the Q-factor of the nanoresonator on the width and length of the beams is then explored. The nanoresonator with the Q-factor over 10^7 is obtainable by eliminating the intrinsic damping mechanisms.

2. The concept of nanoresonator and analysis model

As introduced, TED and anchor losses are the main intrinsic damping sources that affect the upper limit of the Q-factor. For a mechanical resonator, its vibration is composed of flexural and/or torsional components, while TED is caused by flexural vibrations [19]. Flexural vibrations cause alternating tensile and compressive strains on opposite sides of the neutral axis leading to thermal imbalance. The irreversible heat flow, which is driven by the temperature gradient, makes the vibrational energy to be dissipated. Because of the shear strain, the TED loss in a pure torsional vibration is zero, however, in general, a nanoresonator usually includes a mixture of flexure and pure torsion vibrations. On the other hand, anchor loss can be minimized by using the support points with small displacement [15,16]. Taking these two requirements into account, we design an OP vibrational beam nanoresonator as shown in Fig. 1. Two resonant beams with length L_b are connected to two free ends of two spring beams with length $L_s/2$, which oscillate in the torsional mode. The two remaining ends of the two spring beams are connected to the middle of a supporting beam. The dimensional parameters of the nanoresonator are denoted in Fig. 1.

The *Q*-factor of a mechanical resonator is proportional to the ratio of the stored mechanical energy to the dissipated energy per cycle of oscillation. The totally dissipated energy is the sum of energy dissipated by a variety of physical mechanisms. We assume that the nanoresonator is operated under high vacuum conditions. Intrinsic losses including material loss, anchor loss, and thermoelastic damping are remained. The nanoresonator is assumed to be made of single-crystal silicon whose material loss is negligible [30]. In the current design, anchor loss can be eliminated [15]. Therefore, TED is considered to be a dominant damping source.

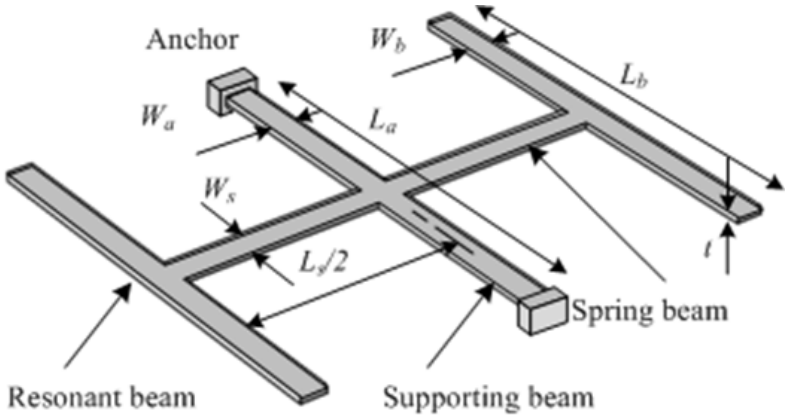

Fig. 1. Schematic drawing of the OP vibrational beam nanoresonator based on the motion transformation mechanism from torsion into rotation

According to the theory of thermoelasticity, the heat transfer equation involving TED is known as

$$\rho C_p \frac{\partial T}{\partial t} - \nabla \cdot (\kappa \nabla T) = -\frac{E\alpha T_0}{1-2\nu}\frac{\partial \varepsilon}{\partial t}, \quad (1)$$

where T is temperature and ε is the elastic strain. The definition and value of other parameters in Eq. (1) are shown in Table 1. The term on the left of Eq. (1) is the heat source showing the heat generation rate per unit volume. ε is defined by

$$\varepsilon = \varepsilon_x + \varepsilon_y + \varepsilon_z = \nabla \cdot u, \quad (2)$$

where u is displacement.

Table 1. Physical parameters of single-crystal silicon used for simulation

Parameters	Definition	Values
E	Young's modulus	165 [GPa]
α	Coefficient of thermal expansion	$2.6e^{-6}$ [1/K]
T_0	Ambient and initial beam temperature	300 [K]
ρ	Density	2330 [kg/m^3]
C_p	Specific heat capacity	700 [J/(kg K)]
C_v	Heat capacity $C_v = \rho C_p$	$1.63x10^6$ [J/(m^{3}K)]
κ	Thermal conductivity	90 [W/(m K)]
ν	Poisson's ratio	0.28

In the theory of dynamics and vibration, the equation of motion is established on the basis of the following force equilibrium:

$$\rho \frac{\partial^2 u}{\partial t^2} = \nabla \cdot \sigma, \quad (3)$$

where σ is the mechanical stress tensor. Furthermore, according to the theory of thermoelasticity, the relation between σ and ε is given by

$$\sigma = C\varepsilon - DT, \quad (4)$$

where *C* is the stiffness matrix and *D* is the thermal expansion coefficient matrix [23].

In harmonic vibration, the temperature *T*, displacement *u*, and velocity *v* have forms as:

$$\begin{cases} T = \Im(xi)\, exp(i\omega t) \\ u = U(xi)\, exp(i\omega t) \\ v = V(xi)\, exp(i\omega t) = i\omega U \end{cases} \quad (5)$$

where ω (= iλ) is the complex angular frequency, which consists of resonant and damping components; $\boldsymbol{\Im(xi)}$, $\boldsymbol{U(xi)}$, and $\boldsymbol{V(xi)}$ are the amplitudes of node temperature, node displacement, and node velocity, respectively.

By substituting Eqs. (2), (4), and (5) into Eqs. (1) and (3), equations for estimating TED in the nanoresonator are given by a 3-order matrix [31]

$$AX = \lambda BX, \quad (6)$$

where *A* and *B* are coefficient matrices, which are derived by applying the standard Galerkin finite element formulation for Eq. (1). The components of matrices *A* and *B* depend on the thermal conductivity *κ*, the density ρ, the specific heat of mass C_p, the elastic modulus *E*, the thermal expansion coefficient α, and Poisson's ratio ν. The eigenvector is $X = (\Im, U, V)^T$, namely a vector combining nodal temperature, displacement, and velocity together. Equation (6) is a generalized eigenvalue equation and the eigenvalue λ is dependent on the representative dimension parameters of the nanoresonator and TED. As presented, the strength of damping caused by TED depends on the structural geometry and also on the material properties which are themselves functions of temperature. It is assumed that the nanoresonator is operated at room temperature. In the following section, the dependence of TED on the representative geometry parameters of the nanoresonator is investigated.

The natural resonant angular frequency $\omega_r$and the *Q*-factor of the nanoresonator according to the real and imaginary parts of λ are as follows [18,23]:

$$\omega_r = |Im(\lambda)|, \quad (7)$$

$$Q = \frac{1}{2}\left|\frac{Im(\lambda)}{Re(\lambda)}\right|, \quad (8)$$

where *Q* is the fraction of energy lost per radian, and the factor 1/2 arises from the fact that the mechanical energy of the nanoresonator is proportional to the square of its amplitude.

To obtain information about the *Q*-factor of the nanoresonator, it is of interest to know its eigenfrequency. To do this, an eigenfrequency analysis is carried out to find eigenvalues. The *Q*-factor of the nanoresonator is calculated by solving the coupled thermoelastic equations by the finite element method in Comsol multiphysics. In this study, the used Comsol module is the MEMS module. The mechanical and thermal problems are coupled through the mechanical and thermal coupling equations as shown in Eq. (6). The mechanical and thermal boundary conditions imposed on the nanoresonator are as follows. Displacement fields at the anchor's boundary is zero and at remained boundaries are free and zero at the initial condition. The nanoresonator is set in an insulated environment and its initial temperature is room temperature. There is no temperature deviation in the nanoresonator at the initial condition. The surfaces of the nanoresonator are set to be thermal isolation conditions. In this research, it is assumed that the nanoresonator is made of single-crystal silicon material. The physical parameters of single-crystal silicon used for simulation are shown in Table 1.

3. Results and discussion

As presented above, nanoresonators oscillating in the pure torsional mode are interested due to negligible thermoelastic damping, which is explained by isovolumetric strain in the pure

torsional oscillation. However, the torsional resonator normally contains flexural vibration components which significantly generate TED [19]. Therefore, the torsional resonator needs to be optimized to obtain the lowest TED, i.e. the highest Q-factor.

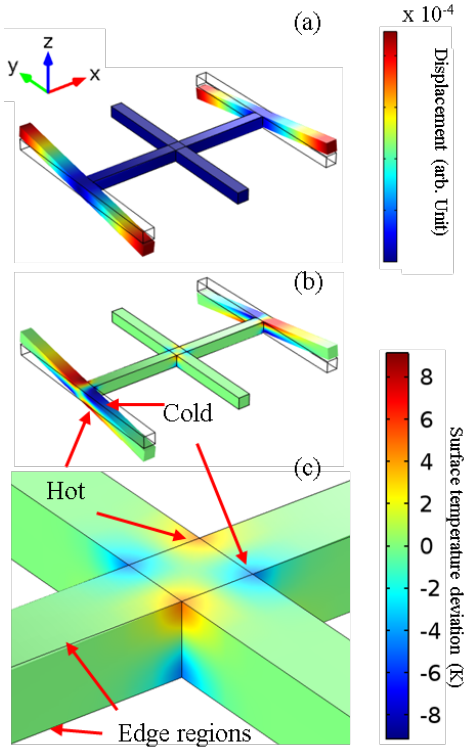

Fig. 2. Perspective view of displacement (a) and temperature distribution (b) of the out-of-phase OP torsional mode of the proposed nanoresonator. In the magnified image of the interconnection between the supporting beam and the torsional spring beam (c), the temperature distribution is clearly seen. The dimensions of the resonant, spring, and supporting beams are $W_{b,s,a}$ = 60 nm, t = 60 nm, and $L_{b,s,a}$ = 1 μm

Figures 2 (a) – (b) show the perspective view and temperature distribution of the nanoresonator in the out-of-phase torsional oscillation mode. This operation mode is the sixth mode of the nanoresonator. As seen in Fig. 2a, the two resonant beams, as well as the two spring beams, oscillate in the out-of-phase mode. Due to the out-of-phase torsional oscillation of the two spring beams, extension and compression regions are periodically distributed around the torsional axis at the four edge regions as shown in Fig. 2c.

For a comprehensively modal analysis, the first five modes of the nanoresonator are also shown in Figs. 3a–e. The resonant frequency f and quality factor Q of the first five modes and the interested sixth mode are presented in Table 2. It is clear that the out-of-phase torsional oscillation mode has a much higher Q value than the remaining modes, except for mode 1. This can be explained that the other modes appear as anchor loss due to the flexural vibration of the spring and supporting beams or the torsional vibration of the supporting beam and TED loss due to the flexural vibration of the spring and supporting beams. Mode 4 is also a torsional mode; however, this torsional mode is the in-phase OP mode, so the moment imbalance occurs at the anchors that cause anchor losses. The moment imbalance also makes the supporting beam to perform flexural vibrations, which causes TED. The anchor and TED losses in mode 4 are the cause that we did not choose for investigating further. For mode 1, its Q value is comparable to that of mode 6; however, the anchor loss of this mode is not negligible due to the displacement of the anchor and the TED loss is caused by the flexural

oscillating spring beam. The resonant frequency of mode 1 is also two times lower than that of mode 6. Moreover, the requirements for high Q nanoresonators are both anchor loss and TED having to be suppressed. Mode 6 fulfills these requirements, so it is chosen for investigation. Therefore, in the following, we will investigate the characteristics of the out-of-phase OP torsional oscillation mode of the nanoresonator. The characteristics of the nanoresonator have been investigated by the finite element method. Here, we have meshed the nanoresonator with the swept mesh method from the top down. This meshing method is chosen due to the symmetrical structure of the nanoresonator. The meshing element is cube-shaped; its size is 20 nm wide × 20 nm long × 6 nm high. The size of such meshing element is suitable for our current calculation facility and acceptable for calculation errors. We have also investigated the convergence of calculation on the meshing size. When we decrease the meshing size from 30 nm to 15 nm, the discrepancy of f and Q is less than 1% and 17 %, respectively.

Table 2. The f and Q values of the first six modes for the nanoresonator with the dimensions of the resonant, spring, and supporting beams $W_{b,s,a}$ = 60 nm, t = 60 nm, and $L_{b,s,a}$ = 1 µm

Mode order	Mode definition	f (MHz)	Q
1	1st out-of-plane cantilever mode	42.113	1.753×10^{7}
2	1st in-plane cantilever mode	61.853	2.385×10^{6}
3	2nd in-plane cantilever mode	76.023	1.593×10^{6}
4	In-phase torsion mode	81.862	9.531×10^{6}
5	2nd out-of-plane cantilever mode	83.911	2.020×10^{6}
6	Out-of-phase OP torsion mode	86.854	2.291×10^{7}

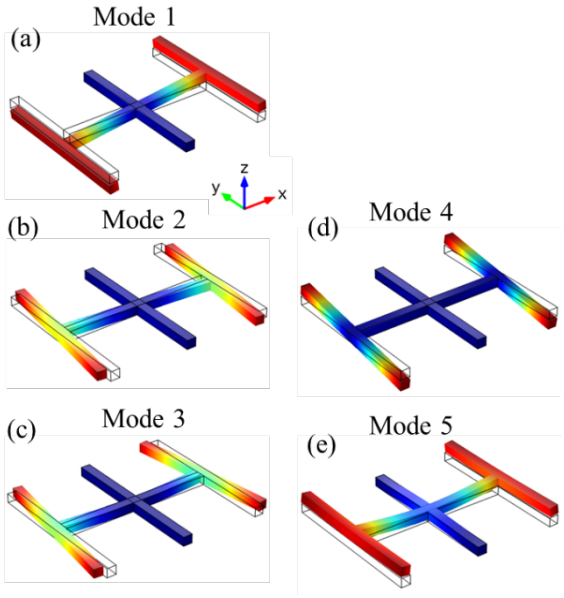

Fig. 3. (a)–(e) show resonant modes from 1–5, which have lower Q than the out-of-phase OP torsional mode, Fig. 2

As above presented, the intrinsic energy dissipation in the nanoresonator is caused by not only TED but also anchor loss. Therefore, it firstly needs to prove that the anchor loss in the nanoresonator in the out-of-phase torsional mode is negligible. It is well-known that the anchor loss is minimal by locating anchors at the stationary points of vibration beams, however, it is challenging to evaluate quantitatively the anchor loss in the nanoresonator having a complex structure. Therefore, we will estimate the anchor loss in terms of investigating TED in the

nanoresonator by decomposing its structure. The anchor loss can be caused by propagating elastic energy through the interconnection between the spring beam and the supporting beam and the two ends of the supporting beam attached to the substrate. To estimate the anchor loss caused by the interconnection between the spring beam and the supporting beam, we compare the *Q*-factor of the asymmetrical nanoresonator as shown in Fig. 4a, which is composed of only half the proposed symmetrical nanoresonator in Fig. 1. The asymmetrical nanoresonator has the *Q*-factor of 1.195×10^7 lower than that of the symmetrical nanoresonator (2.291×10^7). For comparison, the temperature distribution of the asymmetrical nanoresonator is shown in Fig. 4b. Thus, the temperature gradient has appeared in this nanoresonator, which is caused by the extension and compression strain in the flexural vibration of the supporting beam. The supporting beam perform flexural vibrations due to the torsional torque generated by the rotational motion of the spring beam. In contrast, the temperature gradient does almost not appear in the proposed symmetrical nanoresonator, Figs. 2c-d. This means that the anchor loss caused by propagating the elastic energy through the interconnection between the spring beam and the supporting beam is minimized in the proposed symmetrical nanoresonator. It can also be derived from the damping analysis in the asymmetrical and symmetrical nanoresonators that the weakening of the mechanical coupling between the two OP rotating oscillators leads to the increment of TED, i.e. the decrement of the Q-factor. This can be explained that the compression and extension strain of the supporting beam becomes larger when the mechanical coupling strength between the two OP rotating oscillators is weakened.

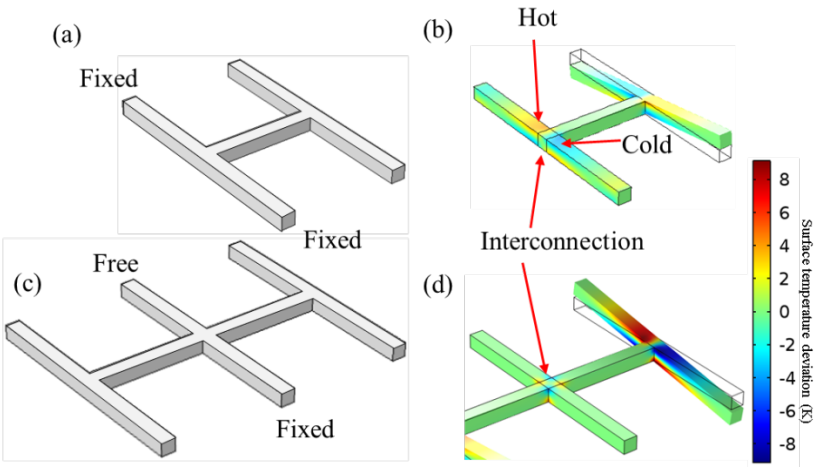

Fig. 4. (a) and (b) are schematic drawings and temperature distributions of the asymmetrical nanoresonator, respectively; (c) and (d) are schematic drawings and temperature distributions of the nanoresonator with one free supporting beam end in the out-of-phase torsion mode, respectively

To estimate the energy dissipation caused by propagating the elastic energy through the two anchors to the substrate, we use the nanoresonator with a fixed-free supporting beam as shown in Fig. 4c. The *f* and *Q* values of this nanoresonator in the out-of-phase torsional mode are almost the same as those of the symmetrical nanoresonator. This can be explained that the torsional spring beam takes the main role in determining the resonant oscillation of both the asymmetric and symmetrical nanoresonators. The deviation of *f* and *Q* of these two nanoresonators are only 4.14×10^{-3} % and 6.25×10^{-2} %, respectively. This also confirms that the out-of-phase torsional oscillation mode does not cause the displacement of the two anchors. Therefore, the elastic energy loss through the two anchors to the substrate is negligible. However, the nanoresonator with the supporting beam clamped at both two ends is considered to

be more robust than that clamped at one end. This is explained due to the higher stiffness of the supporting beam clamped at both two ends.

Thus, by decomposing the structure, we have shown that the anchor loss in the proposed nanoresonator is negligible. Furthermore, we have investigated the same operation mode in the three nanoresonators, the asymmetrical, symmetric, and fixed-free supporting beam nanoresonators, so the relation of the results from the three nanoresonators can be derived. Therefore, the intrinsic energy dissipation is dominant due to TED.

In the following, we will focus on investigating TED in the nanoresonator oscillating in the out-of-phase torsional mode. For the design purpose of one high-Q OP vibrational beam nanoresonator, the dependence of TED on the dimensions of the supporting beam has been investigated. The resonant frequency of the nanoresonator does almost not depend on L_a and W_a. When L_a and W_a increase, the Q-factor of the nanoresonator slightly decreases. This can be explained that the mechanical coupling between the two torsional oscillations on both sides of the supporting beam is being weakened, which leads to the increment of TED.

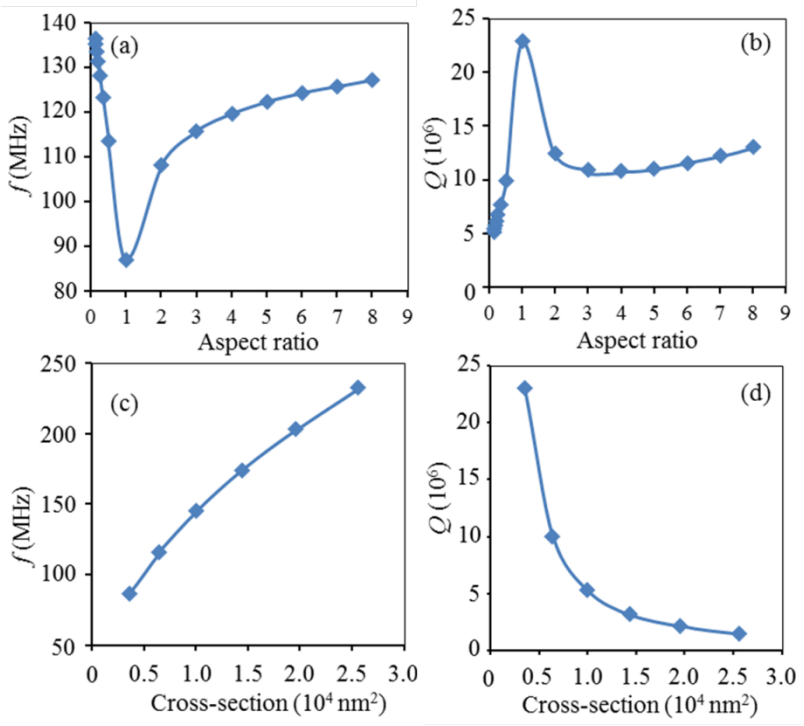

Fig. 5. (a) and (b) are f and Q of the OP vibrational beam nanoresonator investigated as functions of aspect ratio, respectively; (c) and (d) are f and Q of the OP vibrational beam nanoresonator investigated as functions of cross-section, respectively

The f and Q values of the OP vibrational beam nanoresonator have been investigated as a function of the aspect ratio of beams (wide W to thick t ratio). In the investigation, the thickness and length of the beams are fixed at 60 nm and 1μm, respectively, while the width is varied. Figures 5a–b show the investigated results. The frequency response shows an 87 MHz minimum at the aspect ratio of 1, however, the Q-factor obtains a maximum of 2.3×10^7. For the aspect ratio of 1, the Q-factor obtains the highest value. This may be explained that TED in the torsional oscillation with the aspect ratio of 1 is mainly caused by the four edge regions of the torsional oscillation beam and the flexural vibration of the resonant beam. Thus, to maximize the Q-factor of the nanoresonator, the aspect ratio of the spring beam should be chosen to 1, i.e. the cross-section of the spring beam is square-shaped. Based on such criteria, f and Q of the nanoresonator have then been investigated as functions

of cross-section while keeping the aspect ratio to be 1. The investigated results are shown in Figs. 5c–d. f increases with the cross-section, while the Q-factor decreases quickly according to the cross-section. When the cross-section decreases from 2.56×10^4 nm^2 (120 nm wide × 120 nm high) to 36×10^2 nm^2 (60 nm wide × 60 nm high), f decreases a factor of 2.68, however, the Q-factor increases more than one order of the magnitude (16 times).

In the following investigation, the OP vibrational beam nanoresonator with the 60 nm × 60 nm cross-section has the highest Q value chosen to investigate the dependence of Q on L_s. L_s varied from 0.5 μm to 1.75 μm. The investigated results are shown in Fig. 6 (a). The Q-factor strongly depends on L_s. When L_s is varied from 0.5 μm to 1.75 μm, the Q-factor of the OP vibrational beam nanoresonator increases a factor of 5.9 from 8.68×10^6 to 5.15×10^7. In contrast with Q, f decreases a factor of 1.8 from 120 MHz to 66 MHz.

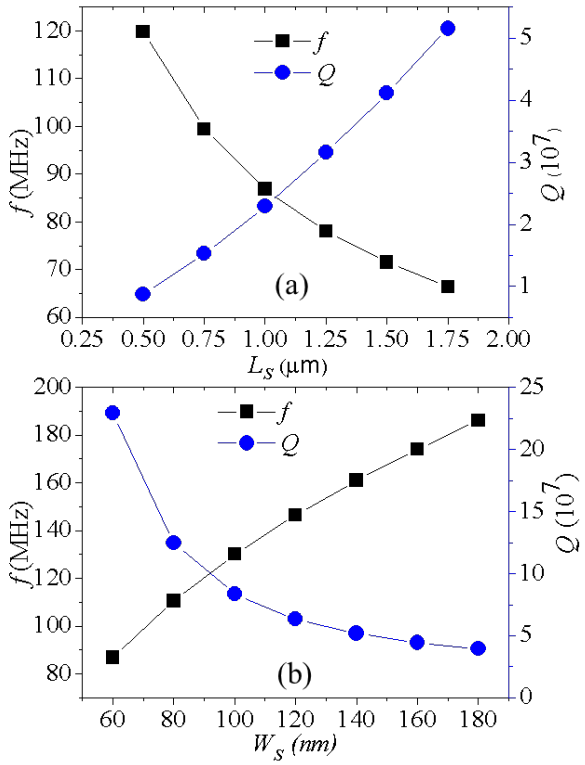

Fig. 6. The resonant frequency and quality factor of the OP vibrational beam nanoresonator were investigated as functions of L_s (a) and W_s (b), respectively

From the investigated result in Fig. 5b, the Q-factor of the OP vibrational beam nanoresonator achieves the maximum value when the aspect ratio of the spring beam is 1. However, for application in practical design, in addition to the study on the Q-factor depending on the length of the spring beam, we have also investigated the Q-factor of the nanoresonator as a function of W_s. In this case, the thickness of the spring beam is kept to be 60 nm, while W_s is varied. The investigated results are shown in Fig. 6b. The Q-factor decreases a factor of 5.8 from 2.29×10^7 to 3.94×10^6, while f increases two times from 86.9 MHz to 186 MHz. Thus, f and Q of the OP vibrational beam nanoresonator strongly depend on the length and width of the spring beam. Here, the spring beam takes part as a torsional oscillation in the nanoresonator. As proved in the previous section, when W_s varies, the aspect ratio of the torsional spring beam differs from 1, this means that TED increases, which leads to the decrement of the Q-factor.

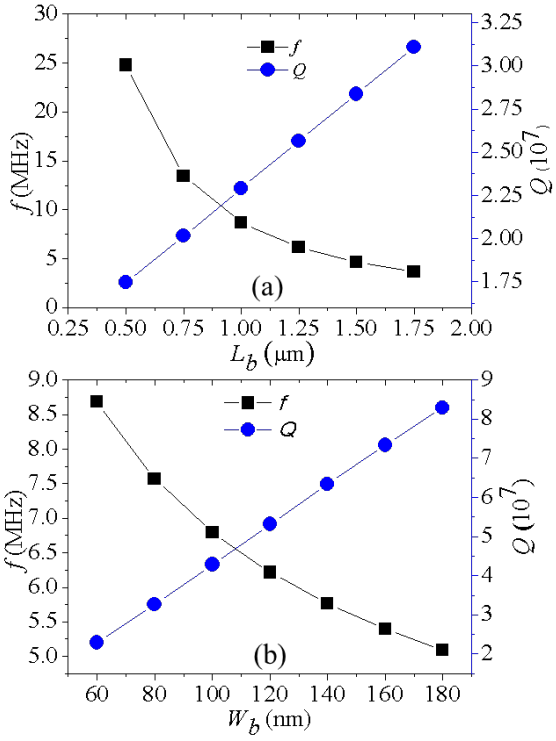

Fig. 7. (a) and (b) show the f and Q of the OP vibrational beam nanoresonator investigated as functions of L_b and W_b, respectively

The f and Q values have also been investigated as functions of L_b and W_b. The results are shown in Figs. 7a - b. As seen in Fig. 7, the Q-factor linearly increases with L_b and W_b. In Fig. 7a, the cross-section of the beams is 60 nm wide × 60 nm high. When L_b increases from 0.5 μm to 1.75 μm, the Q-factor increases a factor of 1.8 from 1.75×10^7 to 3.11×10^7, while f decreases a factor of 6.8 from 248 MHz to 36.6 MHz. When W_b increases from 60 nm to 180 nm (Fig. 7b), the Q-factor increases a factor of 3.6 from 2.29×10^6 to 8.29×10^7, while f decreases a factor of 1.7 from 87 MHz to 51MHz. In this investigation, the thickness of the resonant beam is fixed at 60 nm. The increment of the Q-factor with W_b can be explained by Zener's TED theory [19,20]. The energy distribution exhibits a Lorentzian behavior as a function of $\omega_r\tau$, ($Q^{-1} = \Delta_M (\omega_r\tau/(1 + (\omega_r\tau)^2))$, where, τ $(= \sqrt{\tau_\sigma\tau_\delta})$ is thermal relaxation time, in which τ_σ and τ_δ are the relaxation times of the stress and strain, respectively, Δ_M is a dimensionless quantity called the relaxation strength of the elastic modulus). The energy distribution appears a maximum value when $\omega_r\tau = 1$ [19,20].For the resonating beam with dimensions of 60 nm wide x 60 nm high x 0.5 μm long, τ $(= \rho C_p t^2/\pi^2\kappa)$ is evaluated to be 2.64×10^{-13}, so in the investigated range of W_b, $\omega_r < 1/\tau$. When W_b increases, ω_r decreases due to the increment of the rotational inertia while τ is constant, $\omega_r\tau$ is consequently decreased. Thus, the Q value increases with W_b due to lesser energy dissipated.

4. Conclusion

We have presented the design and simulation analysis of an OP vibrational beam nanoresonator. Based on the motion transformation mechanism from torsion into the rotation, the OP vibrational beam nanoresonator having ultrahigh intrinsic Q-factor in considering both anchor loss and TED is designed and simulated. The torsional oscillation is used to minimize TED, while the out-of-phase vibration is employed to form the stationary points for suppressing anchor loss. The optimal design flow for the OP vibrational beam resonator has been carried out. The torsional spring beam should have a square shape to minimize TED.

The OP vibrational beam nanoresonator with the *Q*-factor over 10^7 is achievable by optimizing its representative geometry parameters.

References

1. Naik AK, Hanay MS, Hiebert WK, Feng XL, Roukes ML. Towards single-molecule nanomechanical mass spectrometry. *Nature Nanotechnology*. 2009;4: 445-450.
2. Xu Y, Lin JT, Alphenaar BW Keynton RS. Viscous damping of microresonators for gas composition analysis. *Applied Physics Letters*. 2006;88(14): 143513.
3. Van Beek JTM, Puers R. A review of MEMS oscillators for frequency reference and timing applications. *Journal of Micromechanics and Microengineering*. 2012;22(1): 013001.
4. Li M, Tang HX, Roukes M. Ultra-sensitive NEMS-based cantilevers for sensing, scanned probe and very high-frequency applications. *Nature Nanotechnology*. 20072: 114-120.
5. Connell ADO, Hofheinz M, Ansmann M, Bialczak RC, Lenander M, Lucero E, Neeley M, Sank D, Wang H, Weides M, Wenner J, Martinis JM, Cleland AN. Quantum ground state and single-phonon control of a mechanical resonator. *Nature*. 2010;464: 697-703.
6. Ilgamov MA. Flexural vibrations of a plate under changes in the mean pressure on its surfaces. *Acoustical Physics*. 2018 64(5): 605-611.
7. Ilgamov MA. Bending and stability of a thin plate under vacuuming its surfaces. *Doklady Physics*. 2018;63(7): 244-246.
8. Ilgamov MA. Frequency spectrum of a wire micro- and nanoresonator. *Doklady Physics*. 2020;65(9): 326-329.
9. Ilgamov MA, Khakimov AG. Influence of pressure on the frequency spectrum of micro- and nanoresonators on hinged supports. *Journal of Applied and Computational Mechanics*. 2021;7(2): 977-983.
10. Hoang MC. Air damping models for micro- and nano-mechanical beam resonators in molecular-flow regime. *Vacuum*. 2016;126: 45-50.
11. Van HD, Van TL, Hane K, Hoang C M. Models for analyzing squeeze film air damping depending on oscillation modes of micro/nano beam resonators. *Archive of Applied Mechanics*. 2021;91(1): 363-373.
12. Bao M, Yang H. Squeeze film air damping in MEMS. *Sensors and Actuators A: Physical.* 2007;136(1): 3-27.
13. Photiadis DM, Judge JA. Attachement losses of high Q oscillators. *Applied Physics Letters*. 2004;85(3): 482-484.
14. Hao Z, Erbil A, Ayazi F. An analytical model for support loss in micromachined beam resonators with in-plane flexural vibrations. *Sensors and Actuators A: Physical*. 2003;109(1-2): 156-164.
15. Kotani S, Hoang CM, Sasaki T, Hane K. Micromirrors connected in series for low voltage operation in vacuum. *Journal of Vacuum Science & Technology B*. 2013;31(4): 42001.
16. Hassani FA, Tsuchiya Y, Mizuta H. Optimization of quality-factor for in-plane free-free nanoelectromechanical resonators. *IET Micro & Nano Letters*. 2013;18(12): 886-889.
17. Taş V, Olcum S, Aksoy MD, Atalar A. Reducing Anchor Loss in Micromechanical Extensional Mode Resonators. *IEEE Transactions on Ultrasonics, Ferroelectrics, and Frequency Control*. 2010;57: 448-454.
18. Yi YB, Matin MA. Eigenvalue Solution of Thermoelastic Damping in Beam Resonators Using a Finite Element Analysis. *Journal of Vibration and Acoustics*. 2007;129(4): 478-483.
19. Zener C. Internal Friction in Solids, I: Theory of Internal Friction in Reeds. *Physical Review*. 1937;52: 230-235.
20. Lifshitz R, Roukes ML. Thermoelastic Damping in Micro- and Nanomechanical Systems. *Physical Review B*. 2000;61: 5600-5609.
21. Bostani M, Karami Mohammadi A. Thermoelastic damping in microbeam resonators

based on modified strain gradient elasticity and generalized thermoelasticity theories. *Acta Mechanica*. 2018;229: 173.
22. Photiadisa DM, Houstona BH, Liu X, Bucaro JA, Marcus MH. Thermoelastic loss observed in a high Q mechanical oscillator. *Physica B*. 2002;316-317: 408-410.
23. Guo X, Yi YB, Pourkamali S. A finite element analysis of thermoelastic damping in vented MEMS beam resonators. *International Journal of Mechanical Sciences*. 2013;74: 73-82.
24. Duwel A, Candler RN, Kenny TW, Varghese M. Engineering MEMS Resonators with Low Thermoelastic Damping. *Journal of Microelectromechanical Systems*. 2006;15: 1437-1445.
25. Guo X, Yi YB. Suppression of thermoelastic damping in MEMS beam resonators by piezoresistivity. *Journal of Vibration and Acoustics*. 2014;333(3): 1079-1095.
26. Losby J, Burgess JAJ, Diao Z, Fortin DC, Hiebert WK, Freeman MR. Thermo-mechanical sensitivity calibration of nanotorsional magnetometers. *Journal of Applied Physics*. 2012;111(7): 07D305.
27. Torres FA, Meng P, Ju L, Zhao C, Blair DG, Liu KY, Chao S, Martyniuk M, Jeune IR, Flaminio R, Michel C. High quality factor mg-scale silicon mechanical resonators for 3-mode optoacoustic parametric amplifiers. *Journal of Applied Physics*. 2013;114(1): 014506.
28. Houston BH, Photiadis DM, Marcus MH, Bucaro JA, Liu X, Vignola JF. Thermoelastic loss in microscale oscillators. *Applied Physics Letters*. 2002;80(7): 1300.
29. Ardito R, Comi C, Corigliano A, Frangi A. Solid damping in micro electro mechanical systems. *Meccanica*. 2008;43: 419-428.
30. Petersen KE. Silicon as mechanical material. *Proceedings of the IEEE*. 1982;70: 420-57.
31. Yi YB. Geometric effects on thermoelastic damping in MEMS resonators. *Journal of Sound and Vibration*. 2008;309: 588-599.

THE AUTHORS

Chu Manh Hoang
e-mail: hoangcm@itims.edu.vn
ORCID: 0000-0001-5808-8736

Nguyen Van Duong
e-mail: manhduong415@gmail.com
ORCID: 0000-0003-3880-9828

Dang Van Hieu
e-mail: hieudv2@fe.edu.vn
ORCID: 0000-0001-7774-775X